Nuclear Physics B121 (1977) 514–530

THE $\pi\pi$ AND $K\bar{K}$ AMPLITUDES, THE S* AND THE QUARK STRUCTURE OF 0^{++} RESONANCES

A.D. MARTIN, E.N. OZMUTLU and E.J. SQUIRES
University of Durham, England

Received 26 July 1976
(Revised 19 January 1977)

The nature of mesons in the 0^{++} nonet is studied. In particular we discuss the parametrization of the $I = 0$ S wave in terms of the S* and possible ϵ mesons. The S* parameters are determined by fitting to $\pi^- p \to \pi^+$ and $K^- K^+$ production data. In particular we find $(g^{S^*}_{KK}/g^{S^*}_{\pi\pi})^2 = 4.0 \pm 0.6$.

1. Introduction

Recent high statistics experiments have provided much new information on the 0^{++} meson nonet. The $I = 1$ member, $\delta(970)$, is seen as a peak in the $\pi\eta$ spectrum just below the $\bar{K}K$ threshold and also as a threshold enhancement in the $K^- K^0$ spectrum (see ref. [1] for recent data and references to earlier observations). The broad κ resonance is seen as the rise through 90° of the, approximately elastic, $I = \frac{1}{2}$ $K\pi$ S wave in the region of 1200 MeV [2]. The structure in the $\pi\pi$ S wave at the KK threshold [3] is attributable to an $I = 0$ S* resonance, and it has been argued [4] that there is in addition a broad ϵ resonance in the $I = 0$ $\pi\pi$ S wave whose mass ($m_\epsilon \sim 1300$ MeV) is consistent with the Gell-Mann-Okubo mass formula for the (δ, κ, ϵ, S*) nonet.

In the L excitation quark model the 0^{++} mesons are an $L = 1$ nonet. Apart from the $L = 0$ ground state 0^{-+} and 1^{--} nonets, the only other nonet for which all the members are observed is the $L = 1$, 2^{++} nonet. The nature and symmetry properties of the 0^{++} nonet are therefore of considerable importance, particularly as many decay channels are experimentally accessible: ϵ, S* $\to \pi\pi$, KK, $\eta\eta$; $\delta \to \pi\eta$, KK and $\kappa \to K\pi$, $K\eta$. The fact that both the S* and δ resonance poles occur just below the KK threshold increases the difficulty of obtaining reliable couplings. For the S* there is the additional complication of the large (ϵ) background.

The main purpose of this paper is to perform a coupled channel ($\pi\pi$, KK) analysis of the $\pi^- p \to \pi^- \pi^+ n$ and $\pi^- p \to K^- K^+ n$ data in the region of the KK threshold, and thereby to obtain a reasonable description of the S*, ϵ effect in the $I = 0$ S wave. The most satisfactory procedure [4] that has been used to describe these overlapping

resonances is to parametrize the Jost function (denoted by $d(s)$ in sect. 2 below). In ref. [4] this is done by writing $d(s)$ as the product of an S* contribution and an ϵ contribution (essentially model IV of our sect. 4). Such a parametrization is hard to interpret from the dynamical viewpoint, and so we consider several alternatives for $d(s)$ motivated by different possible structures of the resonances and see to what extent the data can distinguish between them. This should help illuminate the nature of low-energy resonances.

There is no doubt that one of the most important questions of elementary particle theory is whether the low-energy mesons, for example, are predominantly qq composites as in the simple quark model or whether some, or all, are predominantly meson-meson $\sim$ qqqq states, as in the old 'bootstrap' type models. It could, of course, be the case that they are 'mixed' so that neither extreme is realistic [5]. If the mesons are qq states then in a many-channel model which ignores the quark channels they would have to be inserted as CDD poles. This is obvious and well known if the quarks are real particles whose non-appearance is due to their large mass. If the quarks are permanently confined (as in the MIT bag model, for example ref. [6]) they will never enter into an S-matrix description so their bound states should again appear as elementary particles, i.e. require CDD poles. However, because we have no real understanding of confinement theories, it may be possible to take a contrary view here; see Gustafson et al. [7].

In the work on baryon resonances by the above group [7], who explicitly calculate the left-hand cuts, it is claimed that the low-energy states are meson-baryon composites and that no CDD poles are required. Except for the proviso noted above, this appears to rule out the possibility that those baryons are 3q states as in the simple quark model.

Even within a particular realisation of the quark model this problem is not solved. For instance in the MIT bag model of mesons, in addition to the qq states there are qqqq states with similar masses and indeed the suggestion has been made [8] that the 0^+ mesons considered in this note are of such a type.

It is worth noting that the same problem occurs in the study of the pomeron. In one scheme [9] the non-planar diagrams (the cylinder, etc. of the topological expansion) simply renormalise the f upwards to make a pomeron, whereas in the other (generally referred to as the Harari-Freund scheme, also a property of the dual model) the cylinder itself has a new singularity so that in addition to the (qq) f, etc. there is a ($qq\bar{q}\bar{q}$) pomeron.

The plan of this paper is as follows. In sect. 2 we briefly recall the analytic structure of the S matrix in the two-channel situation and in sect. 3 we consider the parametrization of the δ resonance. In sect. 4 we study the more interesting case of the description of the $I = 0$ S wave in the region of the $K\bar{K}$ threshold. We consider three parametrizations which appear to arise naturally in: (I) a model with a $\pi\pi$ state (ϵ) and a $K\bar{K}$ state (S*) together with a coupling between them, (II) a model with a $\pi\pi$ state (ϵ) and a $q\bar{q}$ state (S*) with no significant force in the KK channel, and (III) a model with no significant forces in the $\pi\pi$ and KK channels and two

states (ϵ, S*) in the qq channels. In a sense that will be made explicit in sect. 5 the results of the analysis of the data appear to rule out III and to favour II over I.

In sect. 5 we describe the coupled channel ($\pi\pi$, K$\bar{\text{K}}$) analysis of the $\pi^- p \to \pi^- \pi^+ n$ and $\pi^- p \to K^- K^+ n$ in the region of the K$\bar{\text{K}}$ threshold. We analyse the data in terms of S, P, D partial waves of the produced di-meson system. We study various parametrizations of the $I = 0$ S wave, including those mentioned above, and determine the S* resonance parameters. In particular, the (sheet II) resonance pole is found to be well determined and independent of the parametrization of the S wave. A discussion of the results is given in sect. 6, together with comments on the status of SU(3) for the 0^{++} nonet and our conclusions.

2. The *S*-matrix

Consider a two-channel situation, for example $\pi\pi$ and KK, and denote the thresholds as $s_1 = 4m_1^2$ and $s_2 = 4m_2^2$, with channel momenta $k_i = \frac{1}{2}(s - s_i)^{1/2}$. The elements of the S matrix, S_{ij}, have right-hand cuts in the s plane starting at s_1 and s_2. As we are only interested in the S wave we omit the subscript I from $\boldsymbol{S}$. We refer to the physical sheet as sheet I; the physical amplitudes are evaluated on the upper side of the right-hand cuts on this sheet. We can define sheets II, III and IV by continuing analytically through the cuts as shown in fig. 1, where, for clarity, we have shown the cuts displaced just below the real axis. Sheets I, II, III, IV correspond to (Im k_1, Im k_2) = ++, −+, −−, +−, respectively.

A convenient way to guarantee the singularity structure and unitarity properties of $\boldsymbol{S}$ is to introduce [10] a real analytic function $d(s) \equiv d(k_1, k_2)$ with square root branch points at $k_1 = 0$ and $k_2 = 0$. Then if we put

$$S_{11} = \frac{d^{\text{II}}(s)}{d^{\text{I}}(s)} = \frac{d(-k_1, k_2)}{d(k_1, k_2)}, \tag{1}$$

$$S_{22} = \frac{d^{\text{IV}}(s)}{d^{\text{I}}(s)} = \frac{d(k_1, -k_2)}{d(k_1, k_2)}, \tag{2}$$

$$S_{11}S_{22} - S_{12}^2 = \frac{d^{\text{III}}(s)}{d^{\text{I}}(s)} = \frac{d(-k_1, -k_2)}{d(k_1, k_2)}, \tag{3}$$

we find that $\boldsymbol{S}$ has the correct analytic structure and is unitary * in the physical region. This method is easily generalised to many channels [10]. The poles of the S matrix are caused by the zeros of $d^{\text{I}}(s) \equiv d(s)$.

We will use the multichannel $\boldsymbol{N}$ over $\boldsymbol{D}$ method and write the S-wave amplitude

$$\boldsymbol{T} = \boldsymbol{N}\boldsymbol{D}^{-1},$$

* This requires also that $|d(-k_1, k_2)| \leq |d(k_1, k_2)|$.

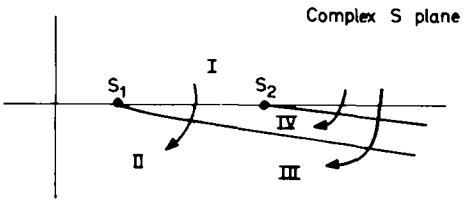

Fig. 1. The sheets reached from the physical sheet, sheet I, by continuing through the right-hand cuts. The cuts are displaced just below real axis for clarity.

where N has the left-hand cuts and D the right-hand cuts. We normalise T so that

$$\text{Im } T = T^* \rho T , \tag{4}$$

$$\rho_{ij} = \theta(s - s_i) k_i \delta_{ij} , \tag{5}$$

hence

$$\text{Im } D = -D\rho N . \tag{6}$$

The real analytic function $d(s)$, introduced above, can be taken to be det $D(s)$. On the physical sheet $d(s)$ does not have the left-hand cuts of S.

3. The ò resonance

We first apply this formalism to the simple case of a single two-channel resonance: the $I = 1$ S-wave δ resonance in the $\pi\eta$ and $K\bar{K}$ channels. We consider the parametrization of this resonance supposing it to be (a) a meson-meson state (we call this exchange model *) and (b) a $q\bar{q}$ state (the quark model).

(a) Exchange model. In this model we assume that the $\pi\eta$ and $K\bar{K}$ exchange forces are responsible for the δ meson. In particular, suppose that forces in the $K\bar{K}$ channel are predominantly responsible for the δ, then we may parametrize D_{22} by a linear function of s and the other elements by constants. We add the threshold terms multiplied by constants. This approximation gives

$$D = \begin{bmatrix} 1 & A - iBk_1 \\ C - iDk_2 & s_R - s - iEk_2 \end{bmatrix} \tag{7}$$

in the resonance region, where A, B, C, D, E and s_R are real parameters. The corresponding N is given by

$$N = \begin{bmatrix} 0 & B \\ D & E \end{bmatrix} , \tag{8}$$

* This is not an ideal name but we follow Gustafson et al. [7] who, like us, were unable to think of a better one.

and the symmetry condition $T_{12} = T_{21}$ requires

$$D = 0 , \qquad B = EC . \tag{9}$$

We therefore obtain

$$d(s) = \det D = m^2 - s - im\Gamma_1 - im\Gamma_2 , \tag{10}$$

with

$$m^2 = s_R - AC , \qquad m\Gamma_1 = EC^2 k_1 , \qquad m\Gamma_2 = Ek_2 . \tag{11}$$

This form of $d(s)$ is the two-channel Breit-Wigner formula.

Note that the form of $d(s)$ would not be different if we put the 'uncoupled' δ in the ππ channel rather than in KK channel. However, if we tried a linear form in both D_{11} and D_{22} (as in model I for the S*, ε in the next section), the fit would require s_{R1} or s_{R2} to be large, so that $d(s)$ would reduce essentially * to form of eq. (10). This is because the data indicate there is no S-wave 'background' to the δ resonance.

(b) Quark model. In this model we assume that the meson-meson forces are weak except *via* the quark channel, MM → qq → MM. In this case we have

$$D = \begin{bmatrix} 1 & 0 & A - iBk_1 \\ 0 & 1 & C - iDk_2 \\ E & F & s_R - s \end{bmatrix} , \tag{12}$$

where the elements in the third row are real, since we are interested in a region well below the qq threshold. It is straightforward to show that $d(s) = \det D$ is once again of the form of eq. (10).

Thus we see that the two models for the δ are indistinguishable and both lead to the Breit-Wigner formula

$$T_{ij} = \frac{mg_i g_j}{d(s)} , \tag{13}$$

where $d(s)$ is given by eq. (10) and $\Gamma_i = k_i g_i^2$. This expression for T_{ij} has poles on sheet III and on sheet II (or sheet IV). We can get an idea about the location of the poles if we ignore the s dependence of the Γ_i. Of course, this is not a reasonable approximation when the poles occur near threshold and so in practice we must solve exactly. However for the purpose of discussion we take $\Gamma_i = \bar{\Gamma}_i \equiv \Gamma_i(m)$. Then the pole nearest the physical region on sheet III is at

$$s = m^2 - im(\bar{\Gamma}_1 + \bar{\Gamma}_2) , \tag{14}$$

* The amplitudes are unchanged if $d(s)$ is multiplied by a real constant.

and that on sheet II (or, if $\Gamma_2 > \Gamma_1$, sheet IV) is at

$$s = m^2 \quad im(\bar{\Gamma}_1 - \bar{\Gamma}_2) . \tag{15}$$

There are also the more distant complex conjugate poles. When the resonance occurs well above both thresholds only the sheet III pole is important. However the δ resonance occurs just below the KK threshold and the 'nearby' sheet II pole is manifest in the $\pi\eta$ mass spectrum.

The $\pi\eta$ mass spectrum has been fitted [1] by this two-channel Breit-Wigner formula with the coupling constant ratio $g^2_{\pi\eta}/g^2_{K\bar{K}}$ fixed at the SU(3) value of $\frac{2}{3}$. The parameters of the δ were found to be

$$m = 974 \pm 9 \text{ MeV} , \qquad \Gamma_{\pi\eta} = 72 \pm 51 \text{ MeV} . \tag{16}$$

These values give a K^0K^- mass spectrum which is in good agreement with the data, when allowance is made for incoherent background effects [1].

Flatté [11] has shown several other Breit-Wigner fits to these $\pi\eta$ and K^0K^- mass spectra and concludes that the data can be fitted almost as well by larger partial widths, $\bar{\Gamma}_{\pi\eta} \sim 300$ MeV. Even with large partial widths the sheet II pole can occur close to the real axis. However, the fall-off of the δ contribution to the KK mass spectrum is a crucial indicator of the sheet III pole position. Although the statistics are low, the K^0K^- spectrum [1] above 1060 MeV suggests that the sheet III pole is closer to the real axis than is permitted by Flatté [11].

For completeness we mention an alternative description of a resonance occurring just below the second threshold, which is based on a constant inverse K-matrix and which has been frequently discussed in the literature [12]. In our notation this parametrization is

$$\boldsymbol{D} = \begin{bmatrix} \alpha - ik_1 & \gamma \\ \gamma & \beta - ik_2 \end{bmatrix} , \tag{17}$$

and therefore $\mathcal{N}$ is the unit matrix. For β small and negative this leads to a sheet II pole just below the (second) $K\bar{K}$ threshold ($k_2 = i|k_2|$) at

$$|k_2| = -\beta + \gamma^2/(\alpha - ik_1) . \tag{18}$$

This pole manifests itself as a resonance in channel 1, which may be called a $K\bar{K}$ bound state resonance. It is easy to show that such a resonance is effectively described by two of the parameters, the third being associated with a background contribution. There is no nearby sheet III pole in this parametrization and so the resonant amplitude T_{12} dies away more slowly ($\sim 1/k_2$) than in the Breit-Wigner description in contradiction with the indications of the data.

4. Parametrization of the S* and ε

Like the δ, the S* resonance occurs just below the $K\bar{K}$ threshold and the sheet II pole is manifest in the structure of the $\pi\pi$ spectrum. However in this case the de-

scription is complicated by the presence of a large, possibly resonant (ϵ), background in the $I = 0$ S wave. We discuss possible parametrizations of this partial wave in the $\pi\pi$, $K\bar{K}$ channels in the region of the KK threshold *.

(I) Exchange model. In this model we assume that the amplitudes are dominated by forces in the $\pi\pi$ and KK channels, together with a coupling between them. We parametrise the diagonal elements of D by linear functions of s and the off-diagonal elements by constants. We add the appropriate threshold terms multiplied by arbitrary constants. Thus,

$$D = \begin{bmatrix} s_\epsilon - s - i\gamma_1 k_1 & A - iBk_1 \\ C - iDk_2 & s_R - s - i\gamma_2 k_2 \end{bmatrix}, \tag{19}$$

which corresponds to an N given by

$$N = \begin{bmatrix} \gamma_1 & B \\ D & \gamma_2 \end{bmatrix}. \tag{20}$$

We calculate $T = ND^{-1}$ and impose the condition that $T_{12} = T_{21}$. This yields

$$B = D, \qquad C = [\gamma_1 A - B(s_\epsilon - s_R)]/\gamma_2 . \tag{21}$$

Thus, for det D we have the 6-parameter form

$$d(s) \equiv \det D = (s_\epsilon - s - i\gamma_1 k_1)(s_R - s - i\gamma_2 k_2) - \frac{1}{\gamma_2}(A - iBk_1)(\gamma_1 A - B(s_\epsilon - s_R) - i\gamma_2 Bk_2) . \tag{22}$$

In the limit in which the $\pi\pi \to$ KK coupling is ignored this model permits a resonance in $\pi\pi$ and one in KK. The former, which we identify with the ϵ, gives the background to the S* state in the $K\bar{K}$ channel.

(II) Mixed model. Here we permit an ϵ background in the $\pi\pi$ state as before, but we do not include any forces in the $\pi\pi \to K\bar{K}$ or $K\bar{K} \to KK$ amplitudes. Instead we include a qq channel in which there is a bound state. Thus

$$D = \begin{bmatrix} s_\epsilon - s - i\gamma_1 k_1 & 0 & A - iBk_1 \\ 0 & 1 & C - iDk_2 \\ E & F & s_3 - s \end{bmatrix}. \tag{23}$$

We have ignored the threshold terms in the $q\bar{q}$ channel since we assume that these are sufficiently distant not to affect the results.

* Here we neglect the K^+K^- and $K^0\bar{K}^0$ mass difference. When detailed threshold mass spectra are available, it will be interesting to study this effect.

When we impose $T_{12} = T_{21}$ we find

$$B = 0\,, \qquad D = -\gamma_1 AF/E\,. \tag{24}$$

We can therefore write

$$d(s) \equiv \det D = (s_\epsilon - s - i\gamma_1 k_1)(s_R - s - i\gamma_2 k_2) - AE\,, \tag{25}$$

which has five effective parameters (s_ϵ, s_R ($\equiv s_3 - CF$), γ_1, γ_2 ($\equiv \gamma_1 AF^2/E$), AE).

We see that this model is identical to model I except that it has the additional restriction that B of model I is zero.

(III) Quark model. Here we ignore all forces in the meson channels and we treat the $\pi\pi \to q\bar{q}$ coupling to lowest significant order. It is convenient to include two $q\bar{q}$ channels (e.g. a $\underline{1}$ and $\underline{8}$ of SU(3)) and parametrize each as a linear function of s. Thus we put

$$D = \begin{pmatrix} 1 & 0 & A + iBk_1 & C + iDk_1 \\ 0 & 1 & E + iFk_2 & G + iHk_2 \\ I & J & s_3 - s & Y \\ K & L & X & s_4 - s \end{pmatrix}. \tag{26}$$

Provided we do not go beyond second order off-diagonal terms, we obtain

$$d(s) \equiv \det D = (s^2 + as + b + ik_1(c + ds) + ik_2(e + fs))\,, \tag{27}$$

where a, b, c, d, e, f are six real constants. Although they both have six parameters, (27) and (22) are different. In particular (27) does not allow any term of the form $(ik_1)(ik_2)$.

In sect. 5 we analyse $\pi^- p \to \pi^- \pi^+ n$, $K\bar{K}n$ data in an attempt to distinguish between the above parametrizations. We also compare with the description obtained by the following parametrizations used in earlier analyses [4,13,14].

(IV) Breit-Wigner and background. In our notation this description means that the S matrix is given by eqs. (1)- (3) with the factorizing form [4]

$$d(s) = d^R(s) d^B(s)\,, \tag{28}$$

where d^R is a two-channel Breit-Wigner form for the S* resonance,

$$d^R(s) = s_R - s - i\gamma_1 k_1 - i\gamma_2 k_2\,, \tag{29}$$

and d^B is the background to the resonance. We take

$$d^B(s) = e^{-ik_1\phi_B}\,, \tag{30}$$

that is we assume a background phase, $\delta_B \equiv k_1\phi_B$, only in the $\pi\pi$ channel. The de-

tails of the fit are found to be independent of the parametrization of δ_B provided it approximates 90° in the S* region. We choose to parametrize δ_B in terms of a broad ππ resonance.

(V) Constant inverse K matrix. In this description the S matrix is calculated using

$$d(s) = (\alpha - ik_1)(\beta - ik_2) - \gamma^2 , \tag{31}$$

see eq. (17), where α, β, γ are the elements of the K^{-1} or M matrix and are real. If α, β, γ are taken to be constant we can get a 3-parameter description of a resonance and background. For example,

$$S_{11} = \left(\frac{ik_2 + \kappa_R^*}{ik_2 + \kappa_R}\right)\left(\frac{\alpha + ik_1}{\alpha - ik_1}\right), \tag{32}$$

where κ_R is the value of $|k_2|$ given in eq. (18). This expression for S_{11} is in the form of resonance (sheet II pole) multiplied by background, where $\delta_B \sim 90°$ provided $|\alpha| \ll k_1$.

5. Analysis of data in the S* region

In order to study the properties of the S* we performed a coupled channel analysis by fitting ππ and $K\bar{K}$ production amplitudes direct to $\pi^- p \to \pi^- \pi^+ n$ and $\pi^- p \to K^- K^+ n$ data. For each reaction we describe the observed moments $\langle Y_M^J \rangle$, with $J \leqslant 2, M \leqslant 1$, of the produced di-meson system in terms of S, P and D waves.

For $\pi^- p \to \pi^- \pi^+ n$ we used the t-channel moments obtained by the CERN-Munich collaboration [15] (see fig. 2). We fitted to data (with $-t < 0.15$ GeV^2) in 20 MeV bins through the range $0.8 < M_{\pi\pi} < 1.2$ GeV using the 'Ochs-Wagner' method [16,17]. That is, the $\pi N \to \pi\pi N$ amplitudes, L_{λ^+}, for producing a ππ system of spin L, helicity λ by ± exchange naturality, are assumed to satisfy (i) $|L_{1+}| = |L_{1-}|$, (ii) $L_{\lambda^+} = 0$ for $\lambda > 1$, (iii) $L_{1-}/L_0 = \sqrt{L(L+1)}/C$ where C is real. We parametrized C as a quadratic function of $M_{\pi\pi}$. The observed moments, with $J \leqslant 2$, are then expressed in terms of L_0, with $L = 0, 1, 2$, and $C(M_{\pi\pi})$.

For $\pi^- p \to K^- K^+ n$ we used the t-channel moments obtained at 6 GeV/c by the Argonne EMS group [18] ($-t < 0.08$ GeV^2) and at 18.4 GeV/c by the CERN-Munich collaboration [19] ($-t < 0.2$ GeV^2). The exchange mechanisms are more complicated in this reaction and to study the $M_{K\bar{K}}$ dependence it is desirable to consider data extrapolated to the π exchange pole. Such a cross-section extrapolation has been done by the CERN-Munich group [19] and so we have normalized all the observed moments to these values. The moments obtained in this way are shown in fig. 3, and are analysed in terms of amplitudes by the 'Ochs-Wagner' method for $M_{K\bar{K}} < 1.15$ GeV.

The observable ππ and $K\bar{K}$ moments are expressed [15–17] in terms of the production amplitudes $L_0(\pi\pi)$ and $L_0(\pi^-\pi^+ \to K^-K^+)$ for $L = 0, 1, 2$, which, in turn,

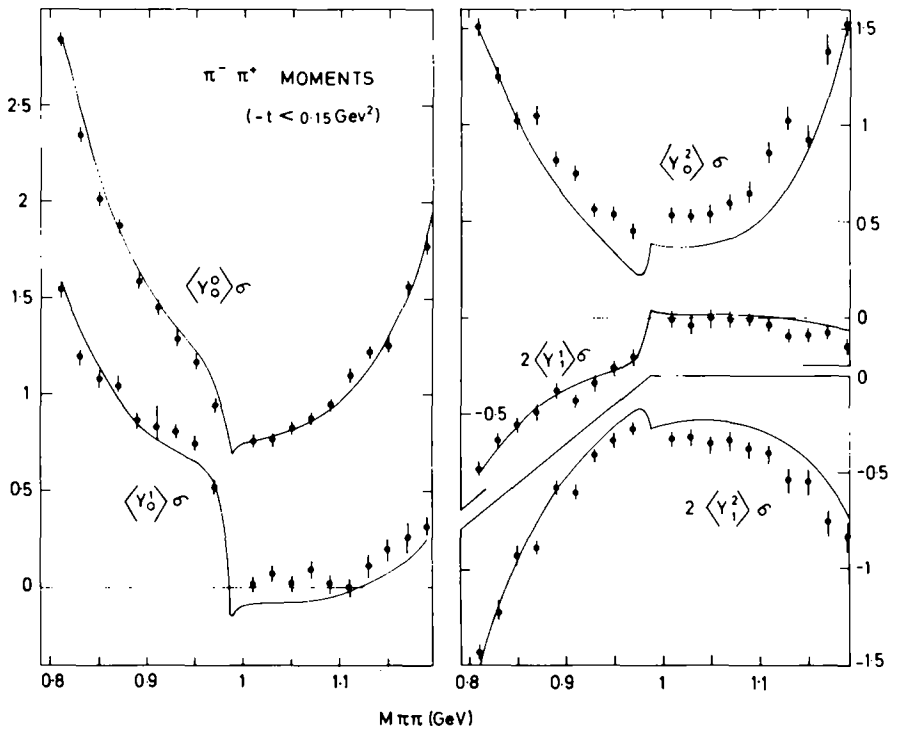

Fig. 2. The mass spectra of the unnormalized t channel $\pi\pi$ moments in the region $0.8 < M_{\pi\pi} < 1.2$ GeV. The data were obtained in the CERN-Munich 17.2 GeV/c $\pi^- p \to \pi^- \pi^+ n$ experiment [15] and correspond to $-t < 0.15$ GeV^2. The curves are the fit using model I.

are given in terms of the S, P, D coupled channel ($\pi\pi$, KK) partial wave amplitudes. We investigated the $I = 0$ S wave parametrizations discussed in sect. 4 by fitting to the data keeping the other partial waves fixed. For the $I = 2$ $\pi\pi$ S wave we input the values of δ_S^2 used in ref. [17] (for example $\delta_S^2 = 22.4°$ at $M_{\pi\pi} = 1$ GeV). For the P and D waves * we used ρ and f resonant forms with the relative $\pi\pi/K\bar{K}$ couplings fixed at their SU(3) values.

The curves on figs. 2 and 3 correspond to the best fit † obtained using the model I parametrization, eq. (22). The parameters obtained are

$$s_R = 0.94 \pm 0.08\,, \qquad \gamma_2 = 0.94 \pm 0.03\,,$$

$$s_\epsilon = 1.4^{+0.9}_{-0.6}\,, \qquad \gamma_1 = 9^{+10}_{-5}\,,$$

$$A = -0.22 \pm 0.42\,, \qquad B = 0.06 \pm 0.55\,, \tag{33}$$

* The small contribution to $\pi\pi$ production from the g resonance tail was also included.

† To allow for the excess of $\pi\pi$, as compared to $K\bar{K}$, production data, we reduced the contribution to χ^2 from the fit to the $\pi\pi$ data by a factor of 4.

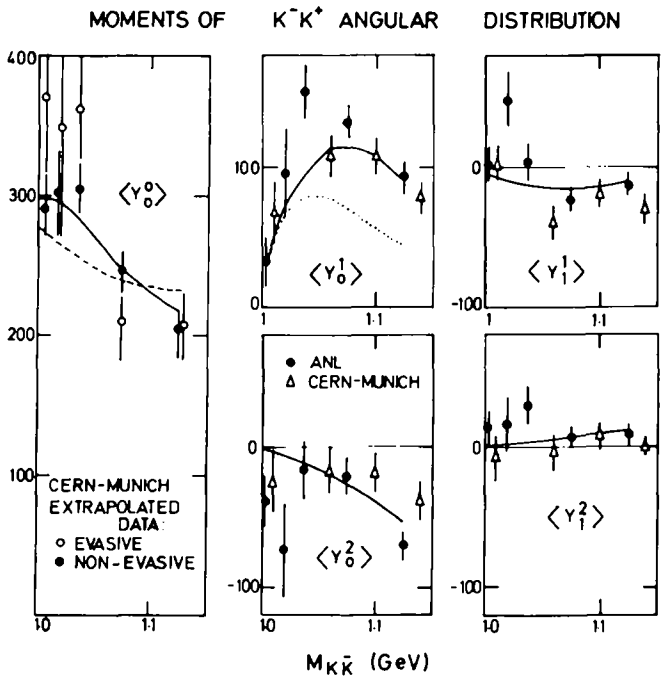

Fig. 3. The t channel moments of the K^-K^+ angular distribution in the reaction $\pi^- p \to K^- K^+ n$. The data for $\langle Y_0^0 \rangle$ are obtained by the CERN-Munich collaboration by extrapolating the cross section to the π exchange pole (see fig. 6 and ref. [19]). All the other moments shown are normalized to these (non-evasive) extrapolated values. The curves correspond to the fit of model I (the dotted line for $\langle Y_0^1 \rangle$ is obtained if the ρ phase is input). The dashed line for $\langle Y_0^0 \rangle$ is the fit using the constant K matrix, model V.

in units of GeV. There are systematic discrepancies in the description of some of the $\pi\pi$ moments which may be due to using fixed Breit-Wigner forms to describe the tails of the ρ and f resonances. Similar systematic misfits in this region were also found [16] in the CERN-Munich phase-shift analysis based on resonance parametrizations. It is interesting to note that if the fit is compared to preliminary Argonne 4 and 6 GeV/c $\pi^- p \to \pi^- \pi^+ n$ data [20] that these discrepancies are reduced *. In the fit we allowed the P wave phase $\delta_P(\pi\pi \to K\bar{K})$ to be free. We found that it was in agreement with that predicted by the tail of the ρ resonance just above the KK threshold, but by $M_{K\bar{K}} = 1.1$ needed to be some 30° larger. If $\delta_P(\pi\pi \to K\bar{K})$ is assumed to be given by the ρ tail, and the other parameters left unchanged, then the dotted curve is obtained for $\langle Y_0^1 \rangle$ for $K\bar{K}$ production, see fig. 3.

The values of four of the six parameters of model I, eq. (33), are poorly deter-

* In particular the ANL data show evidence for the structure indicated for $\langle Y_0^2 \rangle$ at the $K\bar{K}$ threshold.

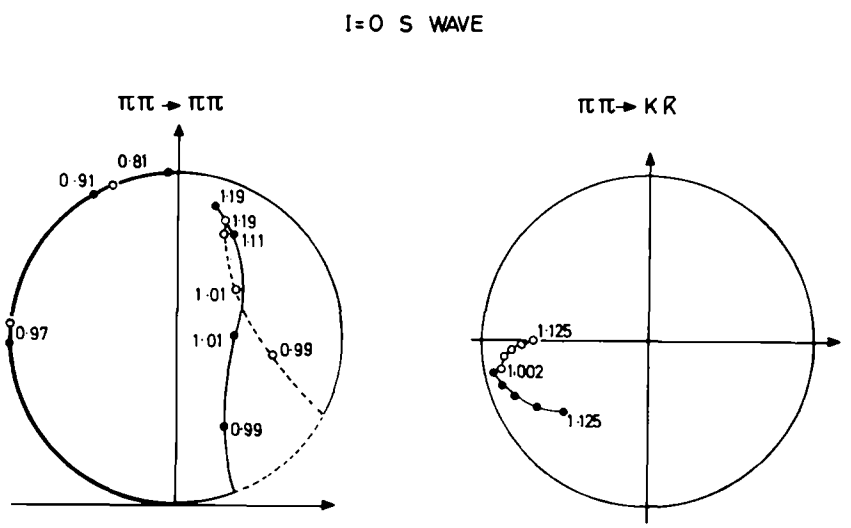

Fig. 4. Argand plots of $k_1 T_{11}$ and $(k_1 k_2)^{1/2} T_{12}$, respectively. The continuous curves, with the mass marked in GeV, are the S wave amplitudes obtained in the fit using model I. Models II and IV give essentially the same amplitudes. The dashed line corresponds to model V. The unmarked points for $\pi\pi \to K\bar{K}$ correspond to $M_{K\bar{K}} = 1.02$, 1.0375, 1.075 GeV respectively.

mined and suggest that the $I = 0$ S wave is over-parametrized. s_ϵ is badly determined because γ_1 is large and the parameters are strongly correlated. As expected from the values of B in eq. (33), model II, which has this $B = 0$, gives essentially the same fit. Moreover model IV, eq. (28), with four effective parameters $s_R = m(S^*)^2$, $\gamma_1 = g^2_{\pi\pi}$, $\gamma_2 = g^2_{K\bar{K}}$ and δ_B * also gives an essentially identical fit, with

$$m(S^*) = 0.978 \pm 0.005\,, \qquad \gamma_1 = 0.199 \pm 0.014\,,$$
$$\delta_B(1\text{ GeV}) = 86.5^\circ\,, \qquad \gamma_2 = 0.792 \pm 0.099\,, \tag{34}$$

in units of GeV.

That such different parametrizations are likely to lead to similar fits can be demonstrated as follows. Since the background phase, δ_B, in model IV is approximately 90° we have

$$d(s) \simeq -i(k_1)(s_R - s - i\gamma_1 k_1 - i\gamma_2 k_2)\,. \tag{35}$$

The introduction of the slowly varying factor (k_1) is irrelevant to the fit, but is required by unitarity. On the other hand for model II the values of the parameters are such that

$$d(s) \simeq -i\gamma_1' k_1 (s_R - s \quad i\gamma_2' k_2) \quad C'\,. \tag{36}$$

* In practice δ_B was parametrized in terms of a broad elastic $\pi\pi$ resonance. The best values were $m(\epsilon) = 1.1$, $g^\epsilon_{\pi\pi} = 3.7$ with very large, strongly correlated errors.

Table 1
The S* pole positions and couplings

Model	Sheet II pole (GeV)	Sheet III pole (GeV)	$(g^{S^*}_{KK}/g^{S^*}_{\pi\pi})^2$
I Exchange	0.997 − *i* 0.017 (±0.002) (±0.002)	0.837 − *i* 0.148 (±0.013) (±0.008)	4.0
II Mixed	0.996 − *i* 0.017 (±0.002) (±0.001)	0.835 − *i* 0.146 (±0.008) (±0.005)	3.9
IV Breit-Wigner	0.996 − *i* 0.016 (±0.003) (±0.002)	0.876 − *i* 0.077 (±0.010) (±0.008)	4.0
V Constant K^{-1} matrix	0.988 − *i* 0.012 (±0.003) (±0.002)		(8.7)

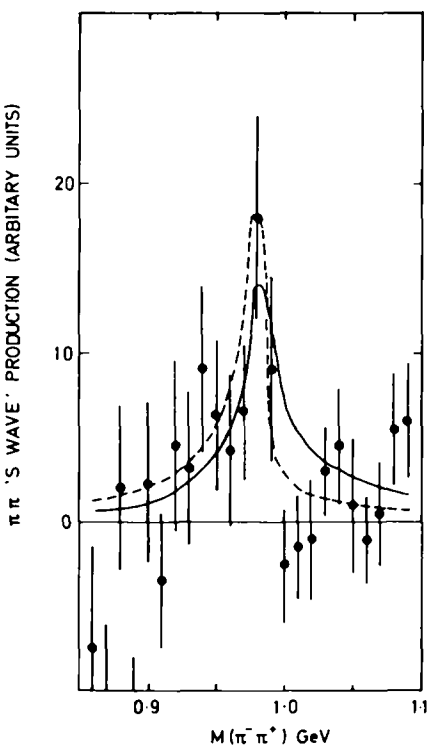

Fig. 5. The $\pi^-\pi^+$ mass distribution observed in $K^-p \to \pi^-\pi^+(\Lambda, \Sigma^0)$ in the S* region with the background and ρ resonance events subtracted [21]. The continuous curve corresponds to the prediction for model I (II, IV) and the dashed curve to that for model V. The curves are proportional to $k_1 M_{\pi\pi}|T_{12}|^2$ and are unnormalized.

To the extent that k_1 is constant over the region of interest, the parametrizations can be seen to be equivalent: $\gamma_2 = \gamma_2'$, $\gamma_1 = C'/k_1^2\gamma_1'$.

We find that model III, eq. (27), is ruled out by the data since it is unable to reproduce the necessary background in the $\pi\pi$ channel. Also the constant inverse K matrix, model V, is unable to give a satisfactory fit to the data. The best fit, using eq. (31), has

$$\alpha = 0.095\,, \qquad \beta = 0.045\,, \quad \gamma = 0.163 \tag{37}$$

in units of GeV, but leads to the behaviour of $\langle Y_0^0 \rangle$ for $K\bar{K}$ production shown by the dashed line in fig. 3. There is only a nearby sheet II pole, and the absence of a nearby sheet III pole does not allow $\langle Y_0^0 \rangle$ to decrease rapidly enough with increasing $M_{K\bar{K}}$ [4,14].

The $I = 0$ S wave amplitudes obtained in the fits are shown in the Argand plots of fig. 4. There is no ambiguity in the sign of the S wave amplitude T_{12} since the interference with the resonance tail contributions is compatible with the $K\bar{K}$ production data provided $g^{S^*}_{K\bar{K}}/g^{S^*}_{\pi\pi}$ is positive [4]. In table 1 we show the S* pole positions corresponding to the various parametrizations. We notice that the sheet II pole position is very stable to changes of the parametrization. We also give the ratio of the S* coupling to the two channels, defined as $|T_{22}/T_{11}|$ at the sheet II pole position.

The S* is also evident in the $\pi\pi$ spectrum observed in the reaction $K^- p \to \pi^-\pi^+(\Lambda, \Sigma^0)$ [21]. The data, with the ρ^0 tail subtracted [21], are shown in fig. 5 together with our predictions for the shape of the spectrum.

6. Discussion and conclusion

We have proposed a form of parametrization of the coupled channel ($\pi\pi$, $K\bar{K}$) $I = 0$ S wave which allows for the presence of overlapping S* and ϵ resonances and which permits an investigation of the nature of these mesons. We found that model III, which we called the quark model, is not able to fit the $\pi^+\pi^-$ and K^+K^- production data. This does not mean, of course, that the S* and ϵ are not predominantly $q\bar{q}$ states, but it does mean that such a description is not simple and that forces in the meson sector are also important. There has to be a significant admixture of meson-meson ($qq\bar{q}\bar{q}$) states in the wave functions. Of course it is not obvious that this makes these resonances any different from the better known ones such as the ρ, since, for example, the observed coupling of the ρ to $\pi\pi$ inevitably mixes a ($qq\bar{q}\bar{q}$) component into its wave function. However, the necessity for such a component has not previously been required experimentally.

Models I and II give satisfactory fits to the data. In the fit with model I a particular parameter turns out to be essentially zero, a fact which is predicted by model II. This gives some evidence in support of model II. However this evidence is very weak as indicated by the errors in (33). The fact that an equivalent fit can be obtained with the four effective parameters of model IV indicates that the S wave is over-pa-

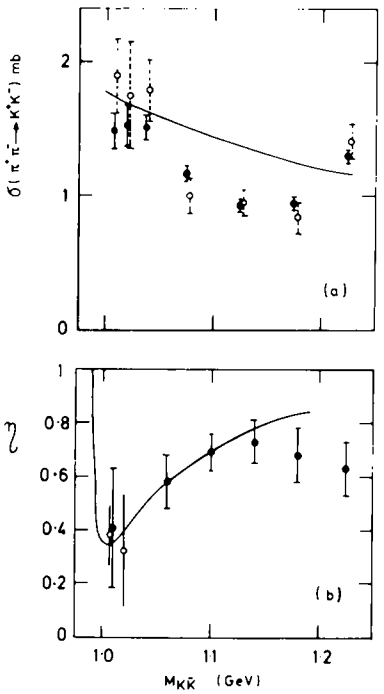

Fig. 6. (a) The $\pi^-\pi^+ \to K^- K^+$ cross section obtained by the CERN-Munich collaboration [19] by extrapolating their 18.4 GeV/c $\pi^- p \to K^- K^+ n$ data to the π exchange pole. The open (closed) points correspond to evasive (non-evasive) extrapolation. The curve is the S wave unitarity limit. (b) The S wave inelasticity, $|S_{11}| = \eta$, obtained from an S, P, D partial-wave analysis of $\pi^- p \to K^- K^+ n$ data [19] normalized to the cross section obtained by the non-evasive extrapolation. The two open points for η are the values obtained assuming only the S wave contributes to the $\pi^-\pi^+ \to K^-K^+$ cross section. The curve corresponds to the model I (II, IV) parametrization.

rametrized in models I and II. Since four S wave parameters suffice to describe the structure of the data in the S* region (three of which are associated with the S*) we are unable to determine meaningful parameters for the ϵ.

Recent $\pi^- p \to K^0_S K^0_S n$ data [22], which contain only even-L $\pi\pi \to K\bar{K}$ partial waves, show evidence for a large S wave under the f resonance. A detailed study of this effect will require a partial wave analysis of data extrapolated to the π exchange pole. Of the recent experiments, the only extrapolated values presently available are those given in the upper part of fig. 6, which shows the $\pi^+\pi^- \to K^+K^-$ cross section obtained by the CERN-Munich collaboration [19] by extrapolation of their $\pi^- p \to K^- K^+ n$ data. We performed an S, P, D wave analysis of the K^+K^- moments [19] for $-t < 0.2$ GeV^2 and calculated the S wave contribution * to the cross sec-

* We show the solution with the larger $|S|$ as required by a study of the $K^0_S K^0_S$ production data [22].

tion. The results are shown in the lower part of fig. 6. The curve corresponds to the model I (II, IV) S wave parametrization. The data indicate that there exists some additional S wave effect for $M_{K\bar{K}} \gtrsim 1.2$ GeV.

If the large S wave under the f resonance is associated with the ϵ then it is at variance with our expectations for SU(3) for the 0^{++} nonet. The SU(3) couplings for the decay of the 0^{++} mesons into two pseudoscalars are given in terms of g_1, g_8 and θ_S, the ϵ - S* mixing angle, in ref. [4]. Note that we define $\Gamma_i = k_i g_i^2$ whereas in ref. [4] Γ_i is essentially $2k_i g_i^2$. Using the δ width to determine * g_8, and using the S* couplings found above, we obtain

$$g_8 = 0.76 \pm 0.2\,, \qquad g_1 = 1.17 \pm 0.2\,, \qquad \theta_S = 68^\circ \pm 15^\circ\,.$$

The ϵ – S* mixing in the 0^{++} nonet is far from ideal [4]. If we use the above values, then SU(3) predicts a broad ϵ resonance in the $\pi\pi$ channel with a very small coupling to the KK channel.

Cerrada et al. [23] have recently discussed $\pi\pi$ and $K\bar{K}$ scattering in the S* region using a different parametrization. They claim that they do not require any nearby resonances. However it is clear that they do not fit the $\pi\pi \to K\bar{K}$ cross section near threshold as shown in our fig. 6 (compare η of their fig. 1). These data are crucial in determining the S* parameters. The claim, that the $KK \to K\bar{K}$ left-hand cut is important, is incorrect since it does not contribute to either T_{11} or $|T_{12}|^2$. In fact this can be seen explicitly using their parametrization: putting $\gamma_{ab} \equiv 0$ in their eq. (8) is found not to affect the results in the S* region.

In summary, we have determined the properties of the S* resonance using $\pi^+\pi^-$ and K^+K^- production data below 1.2 GeV, but are unable to say much about the possible ϵ state in this mass region. The behaviour of the $K\bar{K}$ production data just above threshold are invaluable in determining the S* parameters. Similarly the $(K\bar{K})^{\pm}$ spectra will be crucial for studying the δ. We note that recent $K\bar{K}$ production experiments are finding interesting S wave structure in the region of the f resonance. The high statistics data [24] on the line-reversed reactions $\pi^- p \to K^- K^+ n$ and $\pi^+ n \to K^- K^+ p$ will be invaluable for investigating exchange mechanisms, S* - δ interference and for establishing whether the S wave structure under the f is associated with the $\pi\pi \to K\bar{K}$ channel.

It is a pleasure to thank Drs. P. Estabrooks, D. Morgan, M.R. Pennington, J.L. Petersen and T. Shimada for helpful discussions, and for their interest in this work, and to thank Drs. N.M. Cason, E. Lorenz, A.J. Pawlicki and A.B. Wicklund for communicating and discussing the results of their experiments prior to publication. One of us (E.N.O.) thanks the Turkish Government for financial support.

* The value of g_8 is constrained to be compatible [4] with the behaviour of the $K\pi$ $I = \frac{1}{2}$ S wave phase.

References

[1] J.B. Gay et al., Physics Letters 63B (1976) 220.
[2] T.G. Trippe et al., P.D.G. tables, Rev. Mod. Phys. 48 suppl. (1976) no. 2.
P. Estabrooks et al., contrib. to 18th Int. Conf. on high-energy physics, Tbilisi, 1976.
[3] S.M. Flatté et al., Phys. Letters 38B (1972) 232;
G. Grayer et al., Nucl. Phys. B75 (1974) 189.
[4] D. Morgan, Phys. Letters 51B (1974) 71; New directions in hadron spectroscopy, eds. S.L. Kramer and E.L. Berger, ANL report, p. 45.
[5] E.J. Squires and P.J.S. Watson, Ann. of Phys. 41 (1967) 409.
[6] A. Chodos et al., Phys. Rev. 9 (1974) 3471.
[7] G. Gustafson et al., Nordita preprint 76/5.
[8] R.L. Jaffe and K. Johnson, Phys. Letters 60B (1975) 201.
[9] C. Rosenzweig and G. Chew, Phys. Letters 58 B (1975) 93;
C. Schmid and C. Sorensen, Nucl. Phys. B96 (1975) 209;
H. Lee, Phys. Rev. Letters 30 (1973) 719;
G. Veneziano, Phys. Letters 43B (1973) 413.
[10] K.J. Le Couteur, Proc. Roy. Soc. A256 (1960) 115;
R.G. Newton, J. Math. Phys. 2 (1961) 188;
R. Blankenbecler, Strong interactions and high energy physics, ed. R.G. Moorhouse (1964) p. 411;
M. Kato, Ann. of Phys. 31 (1965) 130.
[11] S.M. Flatté, Phys. Letters 63B (1976) 228.
[12] R.H. Dalitz, Rev. Mod. Phys. 33 (1961) 471;
W.R. Frazer and A.W. Hendry, Phys. Rev. 134 (1964) B1307.
[13] S.D. Protopopescu et al., Phys. Rev. D7 (1973) 1279;
G. Grayer et al., Proc. Tallahassee Conf. AIP Conf. Proc. 13 (1973) 117.
[14] Y. Fujii and M. Fukugita, Nucl. Phys. B85 (1975) 179.
[15] G. Grayer et al., Nucl. Phys. B75 (1974) 189.
[16] W. Ochs, Thesis, University of Munich (1973);
B. Hyams et al., Nucl. Phys. B64 (1973) 134.
[17] P. Estabrooks and A.D. Martin, Nucl. Phys. B79 (1974) 301; B95 (1975) 322.
[18] A.J. Pawlicki et al., Phys. Rev. D12 (1975) 631.
[19] G. Hentschel, Thesis, University of Munich (1976);
E. Lorenz, private communication.
[20] A.B. Wicklund et al., private communication.
[21] G.W. Brandenburg et al., Nucl. Phys. B104 (1976) 413.
[22] N.M. Cason et al., Phys. Rev. Letters 36 (1976) 1485;
W. Wetzel et al., Nucl. Phys. B115 (1976) 208.
[23] M. Cerrada et al., Phys. Letters 62B (1976) 353.
[24] A.J. Pawlicki et al., Phys. Rev. Letters 37 (1976) 971.